molecules

MDPI

Review

Ansa–Ferrocene Derivatives as Potential Therapeutics

Marcin Cybulski [1], Olga Michalak [1], Włodzimierz Buchowicz [2] and Maria Mazur [1,*]

[1] Chemistry Section, Pharmacy, Cosmetic Chemistry and Biotechnology Research Group, Łukasiewicz Research Network–Industrial Chemistry Institute, Rydygiera 8, 01-793 Warsaw, Poland; marcin.cybulski@ichp.lukasiewicz.gov.pl (M.C.); olga.michalak@ichp.lukasiewicz.gov.pl (O.M.)

[2] Faculty of Chemistry, Warsaw University of Technology, Noakowskiego 3, 00-664 Warsaw, Poland; wlodzimierz.buchowicz@pw.edu.pl

* Correspondence: maria.mazur@ichp.lukasiewicz.gov.pl; Tel.: +48-453056174

Abstract: It has been known since the 1990s that the introduction of a ferrocenyl–type substituent into compounds with proven biological activity can improve their properties. More recently, it was also shown that a carbon bridge connecting the two cyclopentadienyl rings in ferrocene derivatives could enhance the biological properties of the new compounds compared to those without them. However, the synthesis of ferrocenes with this additional linker, known as *ansa*–ferrocenes, is more difficult due to advanced synthetic protocols and the phenomenon of planar chirality in ring–substituted compounds. As a result, research into the formation of hybrids, conjugates and other *ansa*–ferrocene derivatives has not been widely conducted. This review discusses the potential biological properties of these units, covering scientific articles published between 1980 and 2024.

Keywords: ferrocene; *ansa*–ferrocene; ferrocenophane; biological activity; anticancer

1. Introduction

Due to their unique physical and chemical properties, structural diversity, ability to ligand exchange, redox and catalytic properties, organometallic compounds represent a promising group of potential drugs [1–3]. Among them, ferrocene and its derivatives have been used in the preliminary development of novel compounds with compelling structures and properties [4]. In the field of bioorganometallic chemistry, the ferrocenyl moiety often serves as a surrogate for functional groups [5,6], usually aromatics, in molecules with established biological activity. Novel compounds synthesized in this way display improved properties when compared to their parent molecules [7–11].

Maintaining a balance between reactive oxygen species (ROS) levels is essential for normal cell function [12,13]. While the presence of ROS had been previously considered detrimental by inducing oxidative stress, some studies have unexpectedly shown that antioxidants could also promote cancer formation and growth [14]. However, it is now accepted that appropriate levels of ROS interfere with normal cell signaling. To fully understand the potential of targeting ROS in cancer therapy, studies of the mechanism of action are essential. Some studies suggest that the mechanism of action of ferrocenes involves reversible redox chemistry and the generation of ROS [15–17]. Released ferrocene complexes can form highly reactive hydroxyl radicals, leading to the generation of ROS [18]. This disrupts the ROS balance via the Fenton pathway, leading to DNA damage and cancer cell death. It has also been shown that the rate of accumulation of ferrocenes in cancer cells is proportional to their cytotoxic activity, i.e., the mechanism responsible for cell death correlates with the transport of ferrocenes into cancer cells. The uptake of ferrocenes into cells is mediated by membrane glycoproteins called transferrin receptors. These receptors are responsible for the cellular uptake of iron from plasma. They can also transport various metal ions and organometallic compounds from the bloodstream to all tissues. This has been demonstrated in a molecular docking study [19]. Although a number of ferrocene

check for updates

Citation: Cybulski, M.; Michalak, O.; Buchowicz, W.; Mazur, M. *Ansa*–Ferrocene Derivatives as Potential Therapeutics. *Molecules* **2024**, *29*, 4903. https://doi.org/10.3390/molecules29204903

Academic Editor: Eike Bauer

Received: 17 September 2024
Revised: 9 October 2024
Accepted: 13 October 2024
Published: 16 October 2024

Copyright: © 2024 by the authors. Licensee MDPI, Basel, Switzerland. This article is an open access article distributed under the terms and conditions of the Creative Commons Attribution (CC BY) license (https://creativecommons.org/licenses/by/4.0/).

derivatives have shown promising biological activity, the potential of *ansa*[n]–ferrocenes (also known as [n]ferrocenophanes) in medicinal chemistry was discovered not long ago. This review discusses the latest developments in research on *ansa*–ferrocenes published in the literature between 1980 and 2024. It includes an analysis of their biological properties, SAR studies and an evaluation of their mechanism of action.

2. Anticancer Properties

2.1. Ferrocenophanes Derived from Ferrocifene Derivatives

Ferrocenophane phenols are a type of ferrocene named after the first published examples of hybrid compounds containing both ferrocene fragments and the anticancer drug tamoxifen [20]. Tamoxifen is a nonsteroidal selective estrogen receptor modulator (SERM) used to treat all stages of hormone receptor–positive breast cancer [21]. Ferrocenyl hydroxytamoxifen **1** as a prototype for a new range of cytostatic agents targeting the estradiol receptor site was published in 1996 (Figure 1) [8]. Ferrocifenes were the first examples demonstrating that the modification of polyphenols with a ferrocenyl substituent can significantly increase cytotoxicity in vitro [22,23]. Although the compounds were designed to target delivery of the cytotoxic ferrocene group to cells overexpressing estrogen receptors, they showed significant in vitro activity against both hormone–dependent MC–7 cells and triple–negative MDA–MB–23 breast cancer cells (IC_{50} = 0.7 μM and IC_{50} = 0.6 for **1**, respectively). These observed antiproliferative effects were much stronger than those of 4–hydroxytamoxifen, the reference antiestrogen and ferrocene alone, which was inactive against these breast cancer lines. However, the recent cytotoxicity values for **1** have been inconsistent with those previously published [24]. The IC_{50}s determined were only 43.3 μM for MCF–7 cells and 26.3 μM for MDA–MB–231 cells after 72 h of incubation. In this study, compound **1** also showed activity against PANC1 pancreatic cancer cells with an IC_{50} of 12.5 μM, twice that of tamoxifen, and significantly increased cellular oxidative stress compared to the reference compound. It is noteworthy that, while promising structures for pancreatic cancer therapy are still being investigated in the case of ferrocene derivatives (see, for example, ferronucleoside, which inhibits DNA replication in a panel of pancreatic cancer cells [25]), no such reports have been published in the case of *ansa*–ferrocenes.

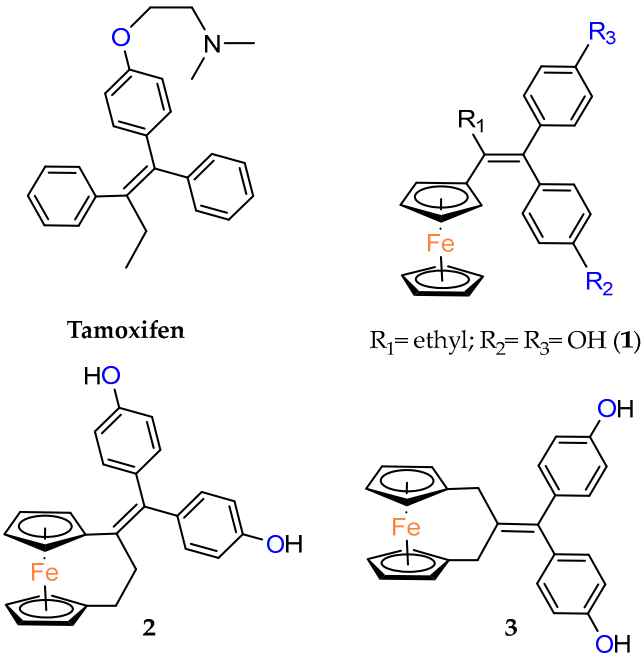


Figure 1. Tamoxifen, ferrocifen (**1**) and its *ansa* derivatives of ferrociphenols.

Over the last three decades, intensive SAR research has led to the discovery of 300 ferrocifenes with various substitutions at the R_1, R_2 and R_3 positions (see Figure 1). Some of these compounds have demonstrated potent anticancer properties against various MDR cancer cell lines, including glioma, metastatic melanoma, breast cancer and leukemia [26]. One direction of synthetic modifications to improve the biological activity of ferrociphenols has been the introduction of carbon, or other atoms containing bridges, linking the two cyclopentadienyl rings in the structure.

Jaouen and coworkers, the leading research group in the synthesis and biological evaluation of ferrocifen analogues, first demonstrated the effect of stiffening structure **1** on biological activity. Two rigid analogues **2** and **3** with cyclopentadienyl rings connected by a three–carbon bridge were designed, synthesized and compared in bioassays with a flexible analogue [27]. Studies of relative binding affinity (RBA) for the estrogen receptor (ER) and activity against breast cancer lines MCF–7 ER+ and MDA–MB–231 ER– and PC–3 prostate cancer cells showed the greatest difference in cytotoxicity of the compounds on hormone–independent MDA–MB–231 and PC–3 cells. (Table 1) Rigid compound **2** was one order of magnitude more cytotoxic than flexible compound **1** or rigid **3,** which lacks conjugation between the phenolic and ferrocenyl groups. Both rigid compounds had estimated cytotoxic activity comparable to **1** for MCF–7 cells. These results suggested that there may be a competition between the positive estrogenic effects and negative cytotoxic effects on this cell line, which could not be predicted from the simple binding values. Compound **4**, with one hydroxyl group, **5** with one amine group in the phenyl ring and **6** with an acetamide substituent showed similar activity against MDA–MB–231, acting less effectively than analogue **2** [28]. Replacement of one hydroxyl in **2** by amine (**8**) or acetamide (**10**) substituents resulted in similarly high activities against MDA–MB–231 with IC_{50} = 0.06 and 0.09 μM, respectively. Compound **11** with one amine group in each phenyl ring also showed high activity. It was in contrast to the result for its acetamide analogue **9**, which acted two orders of magnitude weaker. Interestingly, acetylated prodrug analogues of **2,** i.e., mono acetylated **12** or peracetylated **13**, acted at the level of the leading structure against MD–MB–231 [29,30].

Table 1. Relative binding affinity (RBA) for the estrogen receptor * [27,31].

Compound	RBA (%)	
	ERα	ERβ
1	9.6 ± 0.9	16.3 ± 1.5
2	7.2 ± 0.7	4.84 ± 0.4
3	7.6 ± 0.6	15.4 ± 0.4
31	2.05 ± 0.08	–
33	17.2	–
34	14.4	–
35	4.8	–
38	10.3	–
39	4.4	–

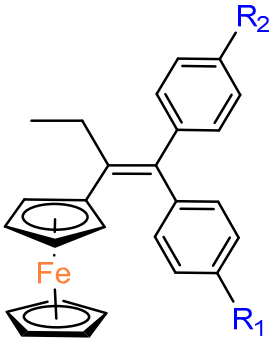
* see structure of compounds in Table 2.

Compound **5** in extended screening in vitro revealed better activity against human glioblastoma SF–295 (IC_{50} = 1.0 μM), human ileocecal colorectal adenocarcinoma HCT–8 (IC_{50} = 0.5 μM) and human promyelocytic leukemia HL–60 (IC_{50} < 0.12 μM) than against melanoma cancer line MDA–MB–435 (IC_{50} > 61.68 μM) derived from the M14 line [32]. Moreover, it showed promising characteristics possessing of high antiproliferative activity and low hemolytic activity on mouse erythrocytes [33].

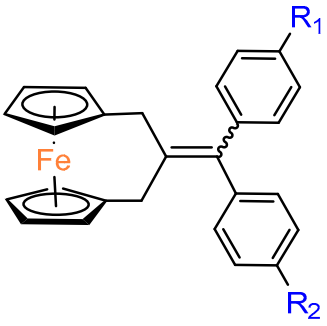
Further study indicated that hybrids **2**, **8**, **10** and **12** could act as DNA alkylating agents or DNA antimetabolites [11,29]. Particularly, hybrid **2** (IC_{50} range 48–580 nM) possessed a broad activity spectrum against a panel of 60 human cancer cell lines, derived from nine different cancer types: leukemia, lung, colon, CNS, melanoma, ovarian, renal, prostate and breast [29,30]. The highest sensitivity of **2** was observed in vitro on human SK–

Mel28 melanoma cells (IC_{50} = 1.2 μM) [26,34]. Compound **2** was also tested on three ovarian epithelial cancer cell lines, including A2780–Cis resistant to cisplatin (IC_{50} = 0.359 μM for A2780; IC_{50} = 0.165 μM for A2780–Cis; IC_{50} = 1.910 μM for SK–OV–3). However, **2** showed a twofold higher selectivity factor (SF = 0.46) against A2780 than the cisplatin–resistant line, when compared to normal human pulmonary fibroblasts MRC5 [35]. The hybrid **2** also showed acceptable acute toxicity in mice, with the maximum tolerated dose of 100 mg/kg. Compound **2** induces senescence in various cancer cell models associated with distinct sensitivity to pro–apoptotic stimuli [36]. The high and broad–spectrum anticancer activity as well as low toxicity made this hybrid a useful starting point in drug development to combat various types of cancers.

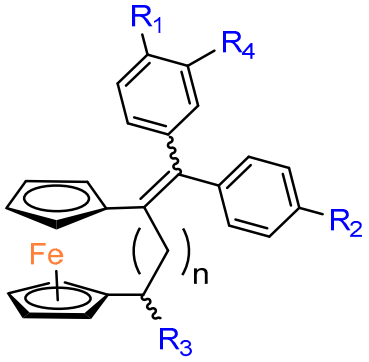
Table 2. Cytotoxicity against breast and prostate cancer lines.



1



3



2, 4-40

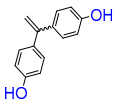
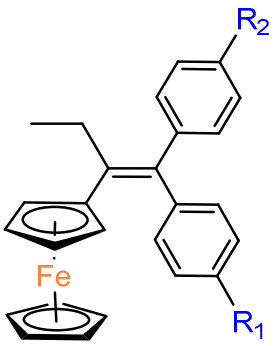
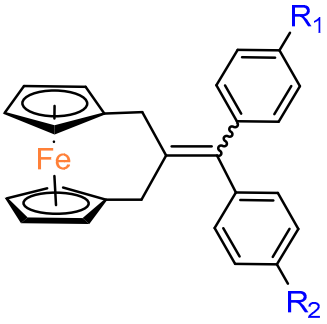
Compound	Ref.	n	R_1	R_2	R_3	R_4	IC_{50} (μM) * MCF–7	MDA–MB–231	PC–3
1	[22]	–	OH	OH	–	–		0.64 ± 0.06	0.7 (1 exp)
2	[27]	1	OH	OH	H	H	4	0.09 ± 0.01	0.094 ± 0.006 or 0.14 ± 0.01 [26]
3	[27]	–	OH	OH	–	–	1	0.96 ± 0.03	1.080.02
4	[28]	1	H	OH	H	H	–	0.47 ± 0.01	–
5	[28]	1	H	NH_2	H	H	–	0.21 ± 0.03	–
6	[28]	1	H	NH–Ac	H	H	–	0.47 ± 0.04	–
7	[29]	1	H	H	H	H		0.92 ± 0.11	2.43 ± 0.47 [26]
8	[29]	1	NH_2	OH	H	H		0.061 ± 0.005	0.03 ± 0.01 [27]
9	[29]	1	NH–Ac	NH–Ac	H	H		5.64 ± 1.13	12.45 ± 0.85 [27]
10	[29]	1	NH–Ac	OH	H	H		0.092 ± 0.019	0.02 ± 0.00 [27]
11	[29]	1	NH_2	NH_2	H	H		0.047 ± 0.010	0.05 ± 0.00 [27]
12	[29]	1	OAc	OH	H	H		0.049 ± 0.003	
13	[29]	1	OAc	OAc	H	H		0.044 ± 0.001	
14	[29]	1	OAc	H	H	H		0.260 ± 0.004	
15	[29]	1	Br	H	H	H		2.93 ± 0.62	
16	[29]	1	Br	Br	H	H		>10	
17	[29]	1	CN	H	H	H		0.85 ± 0.07	
18	[29]	1	CN	CN	H	H		7.98 ± 1.20	
19	[37]	2	OH	OH	H	H		2.41 ± 0.10	
20	[37]	3	OH	OH	H	H		1.85 ± 0.28	
***R*–21**	[37]	1	OH	OH	CH_3	H		0.78 ± 0.12	
***S*–21**	[37]	1	OH	OH	CH_3	H		2.70 ± 0.03	
22	[37]	2	OH	H	H	H		4.53 ± 0.62	
19	[37]	2	OH	OH	H	H		2.41 ± 0.10	
20	[37]	3	OH	OH	H	H		1.85 ± 0.28	
***R*–21**	[37]	1	OH	OH	CH_3	H		0.78 ± 0.12	
***S*–21**	[37]	1	OH	OH	CH_3	H		2.70 ± 0.03	
22	[37]	2	OH	H	H	H		4.53 ± 0.62	
23	[37]	3	OH	H	H	H		4.13 ± 0.18	
24	[37]	3	OH	OH		H		2.70 ± 0.30	

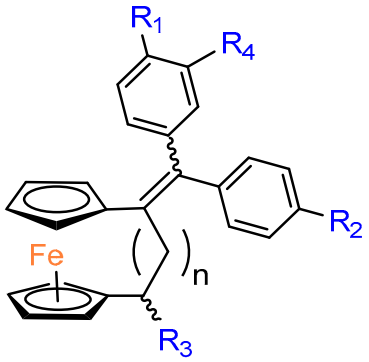
Table 2. *Cont.*



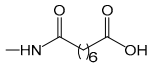
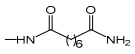
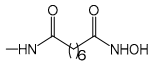
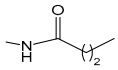
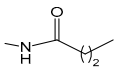
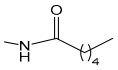
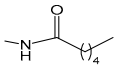
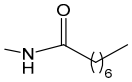
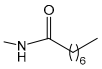
1



3



2, 4-40

Compound	Ref.	n	R_1	R_2	R_3	R_4	IC_{50} (μM) * MCF–7	MDA–MB–231	PC–3
25	[38]	1		H	H	H	4.05 ± 0.57	2.72 ± 0.29	
26	[38]	1		H	H	H	1.78 ± 0.40	0.84 ± 0.28	
27	[38]	1		H	H	H	0.87 ± 0.14	0.94 ± 0.08	
28	[39]	1			H	H		27% **	
29	[39]	1			H	H		23% **	
30	[39]	1			H	H		18% **	
31	[40]	1	$O(CH_2)_3NMe_2$	$O(CH_2)_3NMe_2$	H	H		0.40 ± 0.02	
32	[41]	1	OH	H	H	OH		0.48 ± 0.04	
33	[42]	1	$O(CH_2)_3NMe_2$	OH	H	H		0.18 ± 0.04	
34	[42]	1	$O(CH_2)_3NMe_2$	NH2	H	H		0.17 ± 0.02	
35	[42]	1	$O(CH_2)_3NMe_2$	H	H	H		0.37 ± 0.11	
36	[42]	1	$O(CH_2)_3$pyr	OH	H	H		0.19 ± 0.05	
37	[42]	1	$O(CH_2)_3$pip	OH	H	H		1.10 ± 0.11	
38	[42]	1	$NHCO(CH_2)_2NMe_2$	OH	H	H		0.05 ± 0.02	
39	[42]	1	$NHCO(CH_2)_2NMe_2$	H	H	H		0.39 ± 0.03	
40	[42]	1	$O(CH_2)_4NMe_2$	OH	H	H		0.12 ± 0.06	

* methylene blue assay; after 5 days of incubation, ** percent of cell growth inhibition at 1 mM; pyr = pyridine, pip = piperidine.

Another study was conducted to investigate the impact of the length of the carbon bridge connecting the cyclopentadienyl rings on the activity against MDA–MB–231 cells [37]. The analogues of compound **2** with a four– (**19**) and five–carbon bridge (**20**) exhibited an order of magnitude lower activity than the original structure of **2**. Furthermore, the introduction of an additional methyl substituent into the compound altered its activity. However, the R–isomer (**21**) demonstrated activity similar to that of **2**. The other compound of interest was the relatively bulky derivative of [5]ferrocenophane with two –[bis–(4–hydroxyphenyl)]methylidene groups (**24**). This relatively large compound was still active with an IC_{50} of 2.7 μM [37].

The anticancer activity of hybrid derivatives of superoylanilidine hydroxamic acid (SAHA) having a [3]ferrocenophan–1–ylidene substituent was also evidenced [38]. The compounds **25**, **26** and **27** showed strong antiproliferative activity against triple–negative MDA–MB–231 cells, with IC_{50} values in the 0.84–2.72 μM range. The primary amide **26** was found to be slightly more cytotoxic than its hydroxamide analogue **27**. The cytotoxic effects

of compounds **25–27** were also observed on hormone–dependent MCF–7 breast cancer cells (Table 2), where all three compounds (**25**, **26** and **27**) showed antiproliferative activity with IC_{50} values in the range of 0.87–4.05 μM. In contrary, their analogues lacking the organometallic moiety were unable to inhibit 50% of cell growth even at concentrations of 10 μM. The exception was SAHA (IC_{50} = 1.04 μM), although ferrocenophane hydroxamide **27** (IC_{50} = 0.87 μM) was again slightly more active. In general, incorporation of the ferrocenophane and ferrocene derivatives of hydroxytamoxifene into the suberamide structure enhanced the antiproliferative activity of the resulting compounds against MDA–MB–231 and MCF–7 cancer lines. Of the compounds tested, ferrocenophane derivatives showed the greatest cytotoxicity on MCF–7 breast cancer cells. The electrochemical behavior of these ferrocenophanic suberamides suggested that they undergo redox activation, which may contribute to their antiproliferative activity [38].

The cytotoxic activity of the [3]ferrocenophan–1–ylidene (Fpd) bis–aniline 11 (Fpd, Figure 2) analogues, additionally substituted at the amine groups, was evaluated against hormone–resistant MDA–MB–231 breast cancer cells [39]. The straight dose–dependent effects were not observed for compounds **28**, **29** and **30**. The percentage of cell growth inhibition at concentrations of 1 μM was found to be 27%, 23% and 18%, respectively. The decrease in activity observed for the analogues was accompanied by an increase in the length of the acyl carbon chains. At concentrations one order of magnitude higher (i.e., 10 μM), only compound **29** inhibited the growth of the cancer cell line by more than 50%, reaching 51%. The compounds obtained demonstrated reduced activity compared to the simple diacetanilide derivative **9** (IC_{50} = 5.64 μM). Furthermore, it was demonstrated that modifying the substituents from a basic amine to an amide distinctly diminished the activity against MDA–MB–231 cells. All anilides obtained demonstrated a minimum of two orders of magnitude lower cell growth inhibition when compared to bis–aniline **11** (IC_{50} = 0.05 μM) [39]. The activation mechanism was found to be linked to the intramolecular electron transfer process previously observed for phenolic derivatives. The conversion of Fcpd compounds to ferrocene has been postulated to promote an increase in the ROS level, which can result in direct DNA damage and/or the activation of tumor suppressor genes, leading to apoptosis or senescence of cancer cells [39].

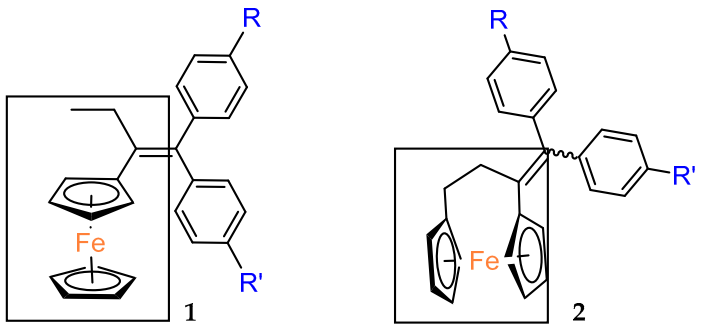


Figure 2. The 1–ferrocenylpropylidene group (Fcpd) and [3]ferrocenophan–1–ylidene group (Fpd).

Replacement of the OH group in **2** by two dimethylaminoalkyloxy chains decreased the cytotoxicity effect on MDA–MB–231 in compound **31** [40]. Against MCF–7 cells, compound **31** showed a slight, but reproducible, proliferative estrogenic effect at low concentrations (1×10^{-8} and 1×10^{-7} M). Following observation on MDA–MB–231 cells, it was very cytotoxic against MCF–7 at higher concentrations (between 1×10^{-7} M and 1×10^{-6} M). According to the binding affinity biochemical studies, **31** appeared highly recognized by the alpha form of ER. While the ability to generate quinone methide formation was blocked in the structure of **31**, an alternative mechanism of its cytotoxicity was investigated in in silico studies. The estimated affinity of the compound to Zn^{2+} and Ca^{2+} indicated the complexing role of two aminoalkyl chains on these cations as a potential mechanism of action [40].

The introduction of an additional hydroxyl group in the *meta* position of the *para*–hydroxyphenyl ring in compound **4** led to a compound **32** with similar biological activity to that of compounds **4**, **6** and **31** (MDA–MB–231 breast cancer cells). The high antiproliferative activity of compound **31** was attributed to the narrower HOMO–LUMO gap present in the oxidized form of [3]ferrocenophane moieties, resulting in more reactive species [41].

A new series of compounds with various aminoalkyloxy side–chains ($O(CH_2)_3NMe_2$, $O(CH_2)_3$piperidine, $O(CH_2)_3$–pyrrolidine, $NHCO(CH_2)_2NMe_2$) were also characterized in terms of their antiproliferative activity against the MDA–MB–231 cancer cells. The IC_{50} values of compounds **33**, **34** and **36** were between 0.17 and 0.19 μM. These values were twice as weak as for the model diphenol **2** (0.09 μM). Nevertheless, these derivatives were among the most efficacious compounds against MDA–MB–23 ever obtained. The lipophilicity of these compounds did not appear to play an important role in their activity. Once again, it was demonstrated that systems lacking an OH group, as in **35** and **39**, are less active. Although, the substitution of the aminoalkoxy chain $–O(CH_2)_3NMe_2$ by the amido chain $NHCO(CH_2)_2NMe_2$ may produce different effects, the IC_{50} values of compounds **35** and **39** were very similar. In contrast, amido compound **38** exhibited three times better cytotoxicity than **33** (IC_{50} = 0.05 μM vs. 0.18 μM), belonging to the most active *ansa*–derivatives ever studied against the MDA–MB–231 cancer cell line. For comparison, molecules **26** and **27** were slightly less effective than compounds **35** and **39**. The lengthening of the amido chain may impact their diminished activity [42]. The in vitro effect of the new complexes **26**, **27** and **33–39** on the growth of MCF–7 hormone–dependent cells was then studied concerning their estrogenic and antiestrogenic properties. The antiestrogenic effect was not observed in the ferrocenophane series **26**, **27** and **33–39**, although a slight estrogenic effect was observed for compounds **33**, **34,** **38** and **39**. The compounds, in general, preserved an affinity for the estrogen receptor. Thus, the estrogenic or antiestrogenic effects were then analyzed exhaustively on the MCF–7 cells for two compounds, **33** and **40**, which differed only in the length of the aminoalkoxy chain. It was investigated at three concentrations (1, 10, 100 nM). Compound **33** triggered an estrogenic effect at 1 nM, which was inverted at a higher concentration of 100 nM due to the appearance of a cytotoxic effect. In contrast, for compound **40**, the antiestrogenic effect started immediately from 1 nM. Therefore, the authors proposed that this phenomenon could be attributed to the length of the aminoalkyl side chain, which may change the estrogenic effect into an antiestrogenic, as was confirmed in the modeling study [42].

Furthermore, the same research group also studied the MDA–MB–231 cell line inhibition growth produced by compounds slightly more different in structure than typical ferrocenophane phenol derivatives (Table 3) [42]. Compounds **48** and **49**, containing a 1,2–diol moiety in the place of a double bond present in model compound **2**, showed the best antitumor properties in the obtained group. The results were comparable to these for their analogues **4** and **7**, i.e., at the 0.1–0.01 μM level of IC_{50}. Moreover, it is interesting to note that two diastereoisomers **49** and **50** differ slightly in their activities.

Table 3. Cytotoxicity against the MDA–MB–231 breast cancer line [31].

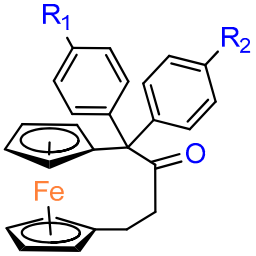
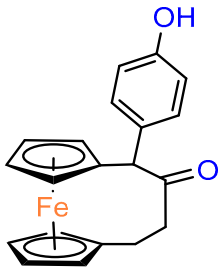
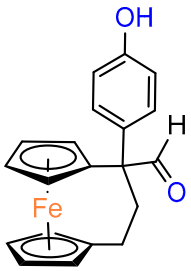
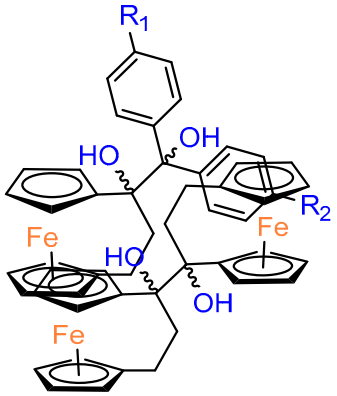
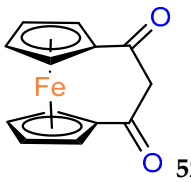
Compound	Structure	R_1	R_2	IC_{50} (μM)
				MDA–MB–231
41		OH	OH	12.5 ± 0.3
42		H	OH	1.45 ± 0.49
43		H	H	20.1 ± 5.4
44		NH_2	NH_2	15.4 ± 0.2
45		NHAc	NHAc	9.38 ± 1.82

Table 3. *Cont.*

Compound	Structure	R_1	R_2	IC_{50} (μM)
				MDA–MB–231
46			No effect at 10^{-5} M	
47			2.83 ± 0.65	
48		H	H	0.17 ± 0.01
49		H	OH	0.06 ± 0.01
50		H	OH	0.14 ± 0.01
51			3.48 ± 0.83	

2.2. Other Ferrocenophanes with All Carbon Bridges

The history of biologically active ferrocenophanes is mainly based on the ferrociphenol derivatives. However, as early as 1980, a simple [3]ferrocenophane–1,3–dione **52** (Figure 3) was tested in vivo against epithelial carcinoma and was found to be inactive [43].



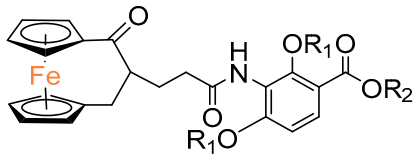
52

Figure 3. [3]Ferrocenophane–1,3–dione.

Another interesting group of compounds was designed to enhance the activity of the antibiotic platensimycin. Although the obtained *ansa*–ferrocene derivatives did not show antimicrobial properties, their intermediates **54** and **55** with protective groups on carboxylic substituents and alternatively on hydroxyl substituents showed in vitro anticancer activity (Table 4). In particular, compound **54**, in which only the carboxyl group was protected

as a 2–(trimethylsilyl)ethyl (TMSE) ester, showed activity at the micromolar level against pancreatic ductal adenocarcinoma PT45 and hepatocellular carcinoma HEPG2 [44].

Table 4. Cytotoxicity of platensimycin derivatives against cancer cell lines [44].



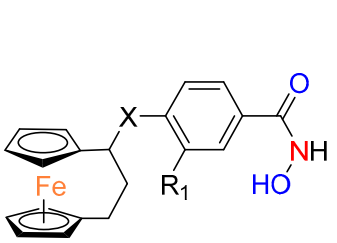
Compound	R_1	R_2	IC_{50} (μM)	
			HepG2	PT45
53	H	H	na	na
54	H	TMSE	3.6 ± 0.2	2.3 ± 0.2
55	Me	Me	48.2 ± 5.8	55.5 ± 2.8

na: no cytotoxic activity up to 200 μM.

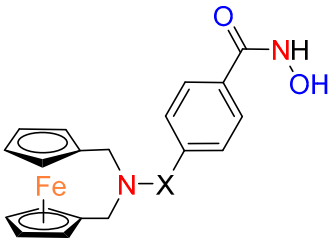
Recently, Yan et al. combined [3]ferrocenophanes and 2–aza–[3]ferrocenophanes **56–64** with benzohydroxamic acid, via a piperazine or piperidine linker, to obtain a new series of ferrocenyl hydroxamic acids (Table 5). Two *ansa*–ferrocene hybrids have shown inhibition of histone deacetylase 6 (HDAC6) at nanomolar concentrations, and this enzyme has been considered a possible target for anticancer and antineurodegenerative therapies [45]. Selected effective inhibitors of HDAC6 were further tested on other HDAC subtypes to identify compound **60** as the most selective to HDCA6 with selectivity ratios, to others from the HDCA family, ranging from 13 to more than 261. Both HDAC6 inhibitors **60** and **63** revealed moderate antiproliferative activity against a panel of cancer cell lines including a prostate cancer cell line (22RV1), an immunoglobulin λ myeloma cell line (MM1.S), a monocyte leukemia cell line (MV4–11), a mantle cell lymphoma cell line (JEKO–1) and a breast cancer cell line (4T1). Compound **63** also induced apoptosis in 4T1 cancer cells in a dose–dependent manner. Western blot studies showed altered levels of proteins involved in the apoptosis pathway under the influence of compound **63**, e.g., PARP or caspase–3. The possible synergism of the pro–apoptotic effects of the compounds was also pointed out by the fact that HDAC inhibitors have the potential to induce apoptosis spontaneously and ferrocene complexes can induce apoptosis through ROS. Thus, this was confirmed by showing an increase in total ROS in 4T1 cancer cells after incubation with **63**.

Buchowicz and coworkers designed and synthesized new uracil–triazole–[4]ferrocenophane hybrids with antitumor activity against breast and lung cancers. The antitumor potential of *ansa*–ferrocene (±)–**65** was evaluated on three cell lines: the hormone–dependent breast cancer cell line MCF–7, the triple–negative breast cancer line MDA–MB–231 and A549 lung cancer cells (Table 6). Compound (±)–**65** acted at the cisplatin level against all cancer lines studied and showed better activity than its nonbridged analogue. The compound also showed significantly lower toxicity against normal MRC–5 cells than cisplatin, particularly in the case of lung cancer A549, where SI for (±)–**65** was 4.2 vs. 1.8 for cisplatin [46].

Table 5. Biological evaluation of compounds **56–64** [45].



56-62



63, 64

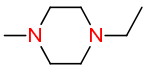
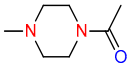
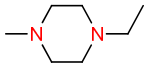
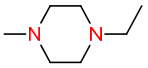
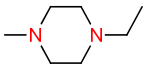
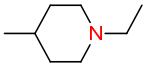
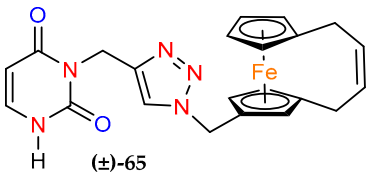
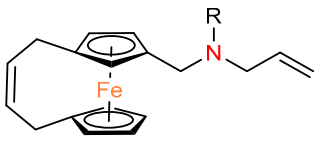
Compound	X	R_1	Inhibition against HDAC6 (IC_{50} (nM))	Antitumor Activities IC_{50} (μM)				
				22RV1	MM1.S	MV4–11	JEKO–1	4T1
56	O	H	545 ± 61					
57	$NHCH_2$	H	534 ± 81					
58		H	200 ± 20					
59		H	635 ± 54					
60		F	38.2 ± 2.1	8.90 ± 2.13	11.90 ± 2.03	7.83 ± 1.62	4.8 0 ± 1.24	16.51 ± 5.13
61		Cl	573 ± 140					
62		OCH_3	2600 ± 376					
63	CH_2	–	76.5 ± 10	8.54 ± 0.50	20.64 ± 4.25	7.73 ± 3.02	10.42 ± 1.98	8.95 ± 1.62
64		–	436 ± 130					

Table 6. Cytotoxicity against cancer cell lines [46,47].



(±)-65



(±)-66, (±)-67

Compound	R	EC_{50} (μM)				
		MCR–5	MCF–7	A–549	PC–3	MDA–MB–231
(±)–**65**	–	45.9 ± 1.5	28.7 ± 2.0	10.9 ± 1.7	–	30.3 ± 4.3
(±)–**66**	H		23 ± 1	71 ± 15	44 ± 13	–
(±)–**67**	CH_3		26 ± 1	68 ± 6	76 ± 15	–

The same research group published a synthesis and biological evaluation of (allylaminomethyl) *ansa*–ferrocene derivatives (±)–**66** and (±)–**67**, which were then compared with their ferrocene analogues [47]. The anticancer effects of (±)–**66** and (±)–**67** were also evaluated against hormone–dependent MCF–7 breast cancer and A–549 lung cancer cells. Furthermore, the compounds were studied using prostate adenocarcinoma PC–3 and mouse noncancerous fibroblasts line Balb 3T3. The tested cell lines showed twice as much sensitivity to *ansa* analogues as their ferrocene counterparts (the same order of magnitude).

Both compounds demonstrated the highest response against MC–7 cells. Compound (±)–**67** was, therefore, administered to examine the effect on the cell cycle progression in this cancer line. The studies showed cycle arrest in the S–phase of DNA replication following administration of increasing concentrations of (±)–**67**. In addition, a sub–G1 phase was observed in MCF–7 cells treated with 40 μM and 60 μM of compound (±)–**67**, indicating the apoptotic nature of an action of (±)–**67**.

2.3. Ferrocenophanes with Bridges Containing Heteroatoms

The biological properties of ferrocenophanes have been tested and demonstrated in several compounds. In addition to the most extensively studied carbon–bridged compounds, the other examples of *ansa*–ferrocenes contain nitrogen (e.g., **63**, **64**), selenium or phosphorus. We note that research on the selenium–bridged compounds is a significant contribution to the broader studies on the bioactivity of different organoselenium derivatives related to their antioxidant and anticancer properties [48].

In studies on allyl derivatives of ferrocene [47], the cytotoxicity of *ansa*–ferrocenes with nitrogen in the bridge was also checked. Compounds **68** and **69** (Figure 4) showed weak activity (EC_{50} > 100 μM) for each of the tested cell lines.

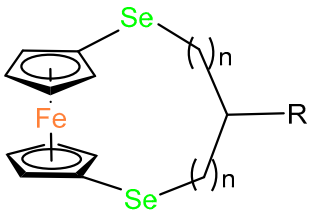


68 **69**

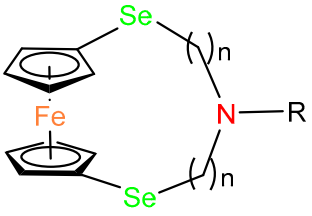
Figure 4. Compounds **68** and **69**.

In studies on the cytotoxicity of organoselenium dopamine conjugates, the *ansa*–ferrocene derivative **70** was found to be the most active in the cytotoxicity assays using AGS (gastric adenocarcinoma), A2780 (ovarian carcinoma), A549 (non–small–cell lung carcinoma), BxPC–3 (pancreatic cancer), HepG2 (hepatocellular carcinoma) and MGC–803 (human gastric cancer) cell lines (Table 7) [49]. HepG2 appeared to be the most sensitive line, with an IC_{50} value of 2.2 ± 0.5 μM. Therefore, the cell cycle distribution in HepG2 was analyzed after administration of 10 or 20 μM of the compound. G1 arrest was observed by indicating a dose–dependent increase in the population of cells in this phase. Subsequently, the population of cells in the S–phase decreased significantly. A dose–dependent presence of cells in the G2/M phase was also observed. Because cell cycle arrest plays a role in apoptosis, the dose–dependent ability of the tested compound to induce apoptosis or necrosis in HepG2 cells was further confirmed by flow cytometry in the presence of annexin stain. The late–stage apoptosis rates of HepG2 cells treated with 10 and 20 μM increased in a dose–dependent manner to 13.09% and 33.62%, respectively. The necrotic rate of HepG2 cells also increased. As a result, compound **70** was effective in directly killing cells or inhibiting the cells growth. Biochemical tests also showed an increase in the pro–apoptotic enzymes caspase 3 and caspase 9. The expression of the pro–apoptotic protein Bax also increased, while a decrease in the anti–apoptotic protein Bcl–2 was observed. Immunoblotting studies also showed an increase in the expression level of the p53 suppressor protein after administration of compound **70**. Encouraging results from in vitro tests led the authors to in vivo experiments, where compound **70** was shown to inhibit tumor growth in nude mice bearing HepG2 tumor xenografts. In addition, **70** inhibited both tubule formation and endothelial cell (HUVEC) migration in the anti–vascular activity assay.

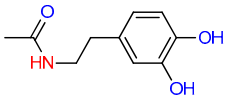
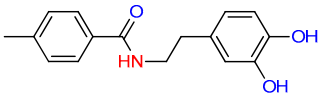
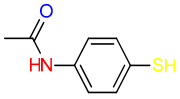
Table 7. Antitumor activities of ferrocenophanes with selenium in the bridge.



70, 72, 73



71

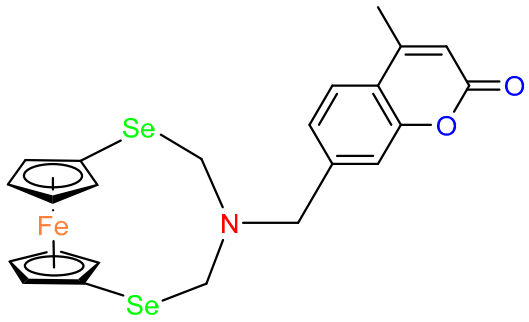
Compound	R	n	Antitumor Activities IC_{50} (μM)					
			AGS	A2780	A549	BX–PC3	HepG2	MGC–803
70		1	2.4 ± 0.4	2.3 ± 0.3	4.8 ± 1.2	5.4 ± 0.7	2.2 ± 0.5	4.5 ± 0.1
71		2	13.2 ± 0.9	21.1 ± 0.7			11.7 ± 0.6	7.8 ± 0.9
72	COOH	1	48.83 ± 2.08 * 99.74 ± 1.06					51.82 ± 3.99 * 91.55 ± 4.15
73		1	220.6 ± 8.7 * 243.1 ± 6.6					243.1 ± 11.0 * 244.4 ± 9.3

* with NIR (near–infrared) light radiation.

Based on the promising results for the seleno–organic derivative of dopamine **70**, a similar dopamine, aza–*ansa*–ferrocene **71,** was obtained among a novel group of compounds. The mechanistic study revealed that the cytotoxicity of these ferrocenyl seleno–dopamine derivatives was mainly related to the Fenton–like reaction under physiological conditions [50].

Core–shell conversion nanoparticles (UCNPs) were functionalized via surface coordination chemistry protocols using *ansa*–ferrocene derivatives **70** and **71** to give conjugates Fc–UCNPs [51]. A drug carrier form (Fc–UCNP) was also obtained by encapsulating Fc–UCNPs in liposomes. It was assumed that the obtained conjugates would be able to release OH radicals in a Fenton–photo reaction activated by NIR radiation to induce cancer cell death. In vitro studies on AGS and MGC–803 cancer lines evidenced the radiation effect in compound **72** (Table 7). None of the two *ansa*–ferrocene derivatives, **72** nor **73**, was selected for further in vitro studies, which demonstrated that the UCNP–Lipo model conjugate, in a xenograft model using AGS cancer cells in BALB/c nude mice, underwent preferential accumulation in a tumor site followed by its enhanced uptake to cancer cells.

To investigate the utility of *ansa*–ferrocene derivatives as compounds with phototriggering properties, a noncovalent complex containing an Eu^{3+} cation and a ClO_4^- anion in the structure of a ferrocenophane derivative with coumarin fluorophore **74** was prepared (Figure 5). In in vitro cell line studies, the compound, which exhibits photoluminescence upon UV irradiation $\geq$ 365 nm, showed phototriggered anticancer activity against HepG2 liver cancer cells, as confirmed by confocal imaging [52].

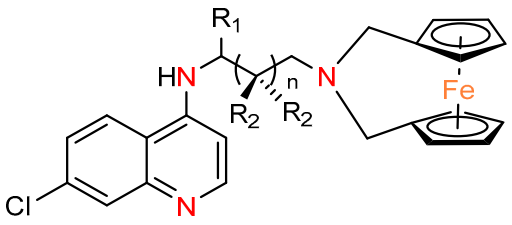


74

Figure 5. Compound 74.

Five ferrocene chloroquine derivatives with the terminal nitrogen of the chloroquine derivative bridging the two cyclopentadienyl rings of ferrocene (**75–79**) were synthesized by Salas et al. [53]. They have been characterized in terms of antiplasmodial activity, as well as cytotoxicity on breast epithelial cells cell line MCF–10A, commonly used as a model for normal human breast cells [54] and melanoma cancer line MDA–MB–435S (but not a breast cancer cell line [55] as mentioned in the cited paper [45]) (Table 8). All tested compounds were found to lower the viability of the cancer cell culture but with low selectivity toward normal cells. Of the series studied, compound **79** appears to be the most active and with the worst selectivity index versus normal line SI = 0.5.

Table 8. Antitumor activities of ferrocenophanes **75–79**.

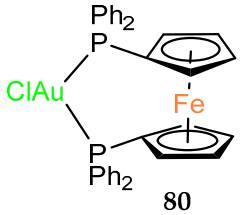


75-79

Compound	n	R_1	R_2	IC_{50} (μM)	
				MCF–10A	MDA–MB–435S
75	0	H	–	2.4 ± 0.2	1.7 ± 0.1
76	1	H	H	4.0 ± 1.0	3.1 ± 0.3
77	2	H	H	4.2 ± 0.9	2.8 ± 0.2
78	0	Me	–	1.4 ± 0.1	1.4 ± 0.1
79	1	H	Me	0.3 ± 0.1	0.6 ± 0.1

Ferrocenophane with a bridge of two phosphorus atoms coordinated to gold(I) was tested in vitro on various cancer cell lines in the 1990s [56]. Compound **80** showed the best activity against the SW1116 cell line (IC_{50} = 48.9 μg mL^{-1}). The cytotoxicity, although improved by the presence of gold, was not better than the cytotoxicity of the well–known drug cisplatin (Table 9).

Table 9. Cytotoxicity of complex **80**.



80

Compound	IC_{50} (μg mL–l)						
	SW620	**SW1116**	**ZR75–1**	**HT1376**	**SKOV–3**	**PA–1**	**LS174T**
80	61.5	48.9	155.7	57.6	66.4	129.0	124.6

3. Miscellaneous Biological Activities Properties of *Ansa*–Ferrocenes

Ansa–ferrocenes **2** and **7** were also investigated as potential blockers of melanin production, for use in cosmetics as compounds that reduce skin pigmentation by acting through a tyrosinase inhibition mechanism [57]. Compound **7**, out of the 20 compounds tested, showed significant inhibition of one of the reactions catalyzed by tyrosinase, i.e., hydroxylation of monophenol (monophenolase activity), by more than 50% at a concentration of 20 μM. In biochemical studies, *ansa*–ferrocene **7** was also classified as a reversible tyrosinase inhibitor.

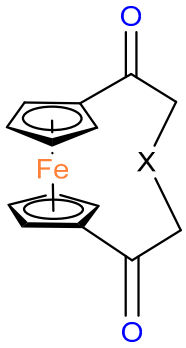
The antiplasmodial activities of compounds **75–79** were evaluated in vitro against the chloroquine–sensitive (CQS) D10 and the chloroquine–resistant (CQR) Dd2 and K1 strains of *P. falciparum* (Table 10). All compounds showed activity against all the tested parasite strains [53]The most active compound of this group is **77** with IC_{50} values of 91.3 and 152.2 nM in the parasite strains D10 and Dd2, respectively.

Table 10. In vitro antiplasmodial activity and resistance indices (RI) against *P. falciparum* CQS D10, CQR Dd2 and CQR K1 strains [49].

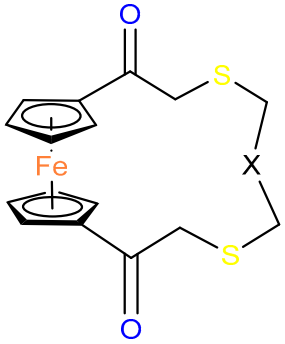
Compound	IC_{50} (nM)			RI	
	CQS D10	**CQR Dd2**	**CQR K1**	**IC_{50} (Dd2)/IC_{50} (D10)**	**IC_{50} (K1)/IC_{50} (D10)**
75	176.0	129.7 ± 23.2	ND	0.7	
76	323.0	224.3 ± 6.73	307.3 ± 170.5	0.7	0.9
77	91.3	152.2 ± 6.52	ND	1.6	
78	444.2	269.2 ± 4.	291.6 ± 2.24	0.6	0.7
79	669.0	506.5 ± 21.	ND	0.7	

Antifungal properties of thia– and aza–ferrocenophanes were also studied. The most promising derivative in this series was found to be the aza–compound **82**, which acted in vitro with an inhibition ratio of 100% for *B. cinerea* and 88.5% for *P. piricola* in the 50 mg/mL concentration (Table 11) [58].

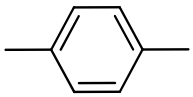
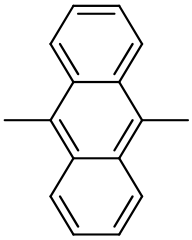
Table 11. The fungicidal activities of thia– and aza–ferrocenophanes [58].



81, 82



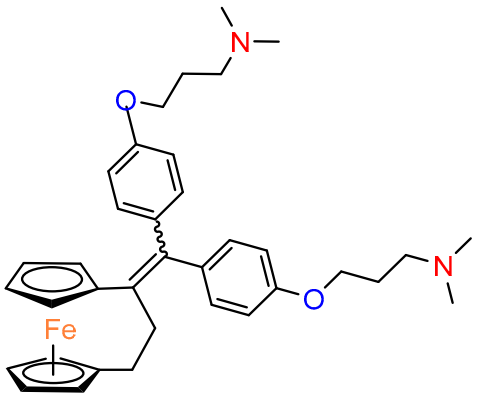
83, 84

Compound	X	Inhibition Ratio (%) (50 μg mL^{-1})			
		A. solani	*C. arachidicola*	*P. piricola*	*B. cinerrea*
81	S	40.0	40.9	68.9	85.7
82	NPh	64.0	50.0	88.5	100
83		56.0	36.4	49.2	78.6
84		60.0	31.8	47.5	71.4

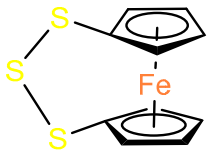
The antibacterial activity of the [3]ferrocenophane phenol analogue (**31**) was studied by el Arbi et al. [59]. Compound **31** was converted to citrate salt to ensure its greater solubility, and then tested against various Gram–positive and Gram–negative foodborne pathogen strains (Table 12). Citrate of **31** was as active as its ferrocenyl counterpart but displayed a twice lower therapeutic index of 0.5 with an HC50 hemolytic activity of 22.4 μM. A [3]ferrocenophane with a sulfur–only bridge has been tested for antimicrobial activity. A variety of bacteria and fungi were used for this study. Compound **85** showed moderate activity (Table 12) [60].

For model compound **2**, which was very active against MDA–MB–231 cancer cells (see the Anticancer Properties section), the evaluation of the antimicrobial activity on the bacteria *Pseudomonas aeruginosa* and *Staphylococcus aureus*, as well as the fungus *Candida albicans* was performed. As a result, no correlation between the antimicrobial, antifungal and anticancer activity was found for **2**. The compound appeared to be inactive against the microorganisms tested [61].

Table 12. Antimicrobial activity of citrate of **31** [50] and **85** [51].



31



85

Strains	MIC (μM)		Diameter of Zone Inhibition (mm)	
	Citrate of 31	85	85	
			30 (μg/disc)	200 (μg/disc)
Listeria ivanovii	12.5			
Listeria monocytogenes	16			
Listeria monocytogenes	8–16			
Enterococcus faecalis	20			
Staphylococcus aureus	8		00	14
Escherichia coli	100, 125	64	00	14
Pseudomonas aeruginosa	>5000		00	16
Salmonella enterica	625			
GM [a] (μM)	41.4			
HC_{50} [b] (μM)	22.4			
TI [c]	0.5			
Bacillus subtilis		64	00	16
Streptococcus β–haemolyticus		64		
Klebsiella species		64	00	16
Salmonella typhi		128	09	17
Shigella dysenteriae			09	18
Candida albicans				10
Aspergillus niger				00
Aspergillus flavus				00

[a] The observed geometric mean (GM) of the MICs of the compound against all bacterial strains. [b] HC_{50} is the minimal concentration that caused 50% hemolysis of red blood cells. [c] Therapeutic index is the ratio of the HC_{50} to the geometric mean of the MICs. Larger values mean greater cell selectivity.

4. Conclusions

Similarly to ferrocene derivatives, ferrocenophanes have attracted interest as compounds with potential anticancer, antibacterial and antifungal properties. The best–known derivative of this group is [3]ferrocenophane phenol **2**, a bridged analogue of flexible ferrocifen **1**. Summarizing, among compounds presented in this review, 61 analogues belong to the [3]ferrocenophane family, thus this structure can be considered the most promising lead for new drug development. However, due to the more complicated synthesis, conformational constraints affecting the outcome of chemical reactions [62], the isolation and purification methods or the phenomenon of planar chirality [63], fewer *ansa*–ferrocene derivatives have been tested so far, at least in preliminary biological tests, when compared to their unbridged analogues. Some reports point to nonscientific problems related to the increasing difficulty of obtaining funding for the development of metallocenes as drugs, including bureaucratic restrictions [64]. Therefore, it appears that compounds from this group

will not easily enter the phase of intensive clinical trials, especially since neither of the two well–known ferrocene derivatives, ferroquine and ferrocifen, have found their way onto the drug market. However, the antimalarial potential of ferroquine is still exploited through various clinical trials testing this compound in combination therapies. For example, the recent contribution of artefenomel to the clinical and parasiticidal activity of ferroquine and artefenomel in uncomplicated Plasmodium falciparum malaria has been investigated [65]. Moreover, the Zydus company applied for a phase I clinical trial of ferroquine and novel triaminopyrimidine ZY–19489 combined therapy against malaria [66].

Author Contributions: Conceptualization, M.C. and M.M.; data curation, M.C., O.M., W.B. and M.M.; writing—original draft preparation, M.C., O.M., W.B. and M.M.; writing—review and editing, M.C., W.B. and M.M.; visualization, M.C., O.M. and M.M.; project administration, O.M. and M.M.; funding acquisition, M.M. All authors have read and agreed to the published version of the manuscript.

Funding: This research was funded by the National Science Centre, grant number 2023/48/C/ST5/00259. WB thanks WUT for financial support.

Conflicts of Interest: The authors declare no conflict of interest.

References

1. Martins, P.; Marques, M.; Coito, L.; Pombeiro, A.J.; Baptista, P.V.; Fernandes, A.R. Organometallic compounds in cancer therapy: Past lessons and future directions. *Anti–Cancer Agents Med. Chem.* **2014**, *14*, 1199–1212. [CrossRef] [PubMed]
2. Hartinger, C.G.; Metzler–Nolte, N.; Dyson, P.J. Challenges and opportunities in the development of organometallic anticancer drugs. *Organometallics* **2012**, *31*, 5677–5685. [CrossRef]
3. Allardyce, C.S.; Dorcier, A.; Scolaro, C.; Dyson, P.J. Development of organometallic (organo–transition metal) pharmaceuticals. *Appl. Organomet. Chem.* **2005**, *19*, 1–10. [CrossRef]
4. Sharma, B.; Kumar, V. Has Ferrocene Really Delivered Its Role in Accentuating the Bioactivity of Organic Scaffolds? *Eur. J. Med. Chem.* **2021**, *64*, 16865–16921. [CrossRef]
5. Jaouen, G. *Bioorganometallics: Biomolecules, Labeling, Medicine*; Wiley–VCH: Weinheim, Germany, 2006.
6. Kowalski, K. Recent developments in the chemistry of ferrocenyl secondary natural product conjugates. *Coord. Chem. Rev.* **2018**, *366*, 91–108. [CrossRef]
7. Biot, C.; Glorian, G.; Maciejewski, L.A.; Brocard, J.S.; Domarle, O.; Blampain, G.; Millet, P.; Georges, A.J.; Abessolo, H.; Dive, D.; et al. Synthesis and antimalarial activity in vitro and in vivo of a new ferrocene−chloroquine analogue. *J. Med. Chem.* **1997**, *40*, 3715–3718. [CrossRef]
8. Top, S.; Tang, J.; Vessières, A.; Carrez, D.; Provot, C.; Jaouen, G. Ferrocenyl hydroxytamoxifen: A prototype for a new range of oestradiol receptor site–directed cytotoxics. *Chem. Commun.* **1996**, *8*, 955–956. [CrossRef]
9. Biot, C.; François, N.; Maciejewski, L.; Brocard, J.; Poulain, D. Bioorganic, Synthesis and antifungal activity of a ferrocene–fluconazole analogue. *Med. Chem. Lett.* **2000**, *10*, 839–841. [CrossRef]
10. Hess, J.; Patra, M.; Pierroz, V.; Spingler, B.; Jabbar, A.; Ferrari, S.; Gasses, R.; Gasser, G. Synthesis, characterization, and biological activity of ferrocenyl analogues of the anthelmintic drug monepantel. *Organometallics* **2016**, *35*, 3369–3377. [CrossRef]
11. Wang, R.; Chen, H.; Yan, W.; Zheng, M.; Zhang, T.; Zhang, Y. Ferrocene–containing hybrids as potential anticancer agents: Current developments, mechanisms of action and structure–activity relationships. *Eur. J. Med. Chem.* **2020**, *190*, 112109. [CrossRef]
12. Bekhet, O.H.; Eid, M.E. The interplay between reactive oxygen species and antioxidants in cancer progression and therapy: A narrative review. *Transl. Cancer Res.* **2021**, *10*, 4196–4206. [CrossRef] [PubMed]
13. Villalpando–Rodriguez, G.E.; Gibson, S.B. Reactive Oxygen Species (ROS) Regulates Different Types of Cell Death by Acting as a Rheostat. *Oxid. Med. Cell. Longev.* **2021**, *2021*, 9912436. [CrossRef] [PubMed]
14. Zhang, V.X.; Sze, K.M.F.; Chan, L.K.; Ho, D.W.H.; Tsui, Y.M.; Chiu, Y.T.; Lee, E.; Husain, A.; Huang, H.; Tian, L.; et al. Antioxidant supplements promote tumor formation and growth and confer drug resistance in hepatocellular carcinoma by reducing intracellular ROS and induction of TMBIM1. *Cell Biosci.* **2021**, *11*, 217. [CrossRef] [PubMed]
15. Osella, D.; Ferrali, M.; Zanello, P.; Laschi, F.; Fontani, M.; Nervi, C.; Cavigiolio, G. On the mechanism of the antitumor activity of ferrocenium derivatives. *Inorg. Chim. Acta* **2000**, *306*, 42–48. [CrossRef]
16. Tabbi, G.; Casssina, C.; Cavigiolio, G.; Colangelo, D.; Ghiglia, A.; Viano, L.; Osella, D. Water stability and cytotoxic activity relationship of a series of ferrocenium derivatives. ESR insights on the radical production during the degradation process. *J. Med. Chem.* **2002**, *45*, 5786–5796. [CrossRef] [PubMed]
17. Hillard, E.; Vessières, A.; Le Bideau, F.; Plazuk, D.; Spera, D.; Huché, M.; Jaouen, G. A series of unconjugated ferrocenyl phenols: Prospects as anticancer agents. *ChemMedChem* **2006**, *1*, 551–559. [CrossRef]
18. Skoupilova, H.; Bartosik, M.; Sommerova, L.; Pinkas, J.; Vaculovic, T.; Kanicky, V.; Karban, J.; Hrstka, R. Ferrocenes as new anticancer drug candidates: Determination of the mechanism of action. *Eur. J. Pharmacol.* **2020**, *867*, 172825. [CrossRef]

19. Güette–Fernández, J.R.; Meléndez, E.; Maldonado–Rojas, W.; Ortega–Zúñiga, C.; Olivero–Verbel, J.; Parés–Matos, E.I. A molecular docking study of the interactions between human transferrin and seven metallocene dichlorides. *J. Mol. Graph. Model.* **2017**, *75*, 250–265. [CrossRef] [PubMed]
20. Jaouen, G.; Vessières, A.; Top, S. Ferrocifen type anti cancer drugs. *Chem. Soc. Rev.* **2015**, *44*, 8802–8817. [CrossRef]
21. Howell, A.; Howell, S.J. Tamoxifen evolution. *Br. J. Cancer* **2023**, *128*, 421–425. [CrossRef]
22. Vessières, A.; Top, S.; Pigeon, P.; Hillard, E.; Boubeker, L.; Spera, D.; Jaouen, G. Modification of the estrogenic properties of diphenols by the incorporation of ferrocene. Generation of antiproliferative effects in vitro. *J. Med. Chem.* **2005**, *48*, 3937–3940. [CrossRef] [PubMed]
23. Nguyen, A.; Vessières, A.; Hillard, E.A.; Top, S.; Pigeon, P.; Jaouen, G. Ferrocifens and ferrocifenols as new potential weapons against breast cancer. *Chimia* **2007**, *61*, 716–724. [CrossRef]
24. Kalabay, M.; Szász, Z.; Láng, O.; Lajkó, E.; Pállinger, É.; Duró, C.; Jernei, T.; Csámpai, A.; Takács, A.; Kőhidai, L. Investigation of the Antitumor Effects of Tamoxifen and Its Ferrocene–Linked Derivatives on Pancreatic and Breast Cancer Cell Lines. *Pharmaceuticals* **2022**, *15*, 314. [CrossRef]
25. Rana, M.; Perotti, A.; Bisset, L.M.; Smith, J.D.; Lamden, E.; Khan, Z.; Ismail, M.K.; Ellis, K.; Armstrong, K.A.; Hodder, S.L.; et al. A ferrocene–containing nucleoside analogue targets DNA replication in pancreatic cancer cells. *Metallomics* **2022**, *14*, 41. [CrossRef]
26. Idlas, P.; Lepeltier, E.; Jaouen, G.; Passirani, C. Ferrocifen Loaded Lipid Nanocapsules: A Promising Anticancer Medication against Multidrug Resistant Tumors. *Cancers* **2021**, *13*, 2291. [CrossRef]
27. Plazuk, D.; Vessières, A.; Hillard, E.A.; Buriez, O.; Labbé, E.; Pigeon, P.; Plamont, M.A.; Amatore, C.; Zakrzewski, J.; Jaouen, G. A [3]ferrocenophane polyphenol showing a remarkable antiproliferative activity on breast and prostate cancer cell lines. *J. Med. Chem.* **2009**, *52*, 4964–4967. [CrossRef]
28. Gormen, M.; Plazuk, D.; Pigeon, P.; Hillard, E.A.; Plamont, M.A.; Top, S.; Vessières, A.; Jaouen, G. Comparative toxicity of [3]ferrocenophane and ferrocene moieties on breast cancer cells. *Tetrahedron Lett.* **2010**, *51*, 118–120. [CrossRef]
29. Görmen, M.; Pigeon, P.; Top, S.; Hillard, E.A.; Huché, M.; Hartinger, C.G.; de Montigny, F.; Plamont, M.A.; Vessières, A.; Jaouen, G. Synthesis, Cytotoxicity, and COMPARE Analysis of Ferrocene and [3]Ferrocenophane Tetrasubstituted Olefin Derivatives against Human Cancer Cells. *ChemMedChem* **2010**, *5*, 2039–2050. [CrossRef]
30. Görmen, M.; Pigeon, P.; Top, S.; Vessières, A.; Plamont, M.A.; Hillard, E.A.; Jaouen, G. Facile synthesis and strong antiproliferative activity of disubstituted diphenylmethylidenyl–[3]ferrocenophanes on breast and prostate cancer cell lines. *MedChemComm* **2010**, *1*, 149. [CrossRef]
31. Görmen, M.; Pigeon, P.; Hillard, E.A.; Vessières, A.; Huché, M.; Richard, M.-A.; Mcglinchey, M.J.; Top, S.; Jaouen, G. Synthesis and Antiproliferative Effects of [3]Ferrocenophane Transposition Products and Pinacols Obtained from McMurry Cross–Coupling Reactions. *Organometallics* **2012**, *31*, 5856–5866. [CrossRef]
32. Rae, J.M.; Creighton, C.J.; Meck, J.M.; Haddad, B.R.; Johnson, M.D. MDA–MB–435 cells are derived from M14 Melanoma cells—A loss for breast cancer, but a boon for melanoma research. *Breast Cancer Res. Treat.* **2007**, *104*, 13–19. [CrossRef] [PubMed]
33. de Oliveira, A.C.; Hillard, E.A.; Pigeon, P.; Rocha, D.D.; Rodrigues, F.A.R.; Montenegro, R.C.; Costa–Lotufo, L.V.; Goulart, M.O.F.; Jaouen, G. Biological evaluation of twenty–eight ferrocenyl tetrasubstituted olefins: Cancer cell growth inhibition, ROS production and hemolytic activity. *Eur. J. Med. Chem.* **2011**, *46*, 3778–3787. [CrossRef] [PubMed]
34. Besnier, P.; Galopin, N.; Sibiril, Y.; Clavreul, A.; Cayon, J.; Briganti, A.; Legras, P.; Vessières, A.; Montier, T.; Jaouen, G.; et al. Efficient ferrocifen anticancer drug and Bcl–2 gene therapy using lipid nanocapsules on human melanoma xenograft in mouse. *Pharmacol. Res.* **2017**, *126*, 54–65. [CrossRef]
35. Pigeon, P.; Wang, Y.; Top, S.; Najlaoui, F.; Garcia Alvarez, M.C.; Bignon, J.; McGlinchey, M.J.; Jaouen, G.A. New Series of Succinimido–ferrociphenols and Related Heterocyclic Species Induce Strong Antiproliferative Effects, Especially against Ovarian Cancer Cells Resistant to Cisplatin. *J. Med. Chem.* **2017**, *60*, 8358–8368. [CrossRef]
36. Bruyère, C.; Mathieu, V.; Vessières, A.; Pigeon, P.; Top, S.; Jaouen, G.; Kiss, R. Ferrocifen derivatives that induce senescence in cancer cells: Selected examples. *J. Inorg. Biochem.* **2014**, *141*, 144–151. [CrossRef]
37. Beauperin, M.; Top, S.; Richard, M.A.; Plażuk, D.; Pigeon, P.; Toma, S.; Poláčková, V.; Jaouen, G. The length of the bridging chain in *ansa*–metallocenes influences their antiproliferative activity against triple negative breast cancer cells (TNBC). *Dalton Trans.* **2016**, *45*, 13126–13134. [CrossRef] [PubMed]
38. Cázares–Marinero, J.D.J.; Buriez, O.; Labbé, E.; Top, S.; Amatore, C.; Jaouen, G. Synthesis, characterization, and antiproliferative activities of novel ferrocenophanic suberamides against human triple–negative MDA–MB–231 and hormone–dependent MCF–7 breast cancer cells. *Organometallics* **2013**, *32*, 5926–5934. [CrossRef]
39. de Jesús Cázares–Marinero, J.; Labbé, E.; Top, S.; Buriez, O.; Amatore, C.; Jaouen, G. The effect of protic electron donor aromatic substituents on ferrocenic and [3]ferrocenophanic anilines and anilides: Some aspects of structureeactivity relationship studies on organometallic compounds with strong antiproliferative effects. *J. Organomet. Chem.* **2013**, *744*, 92–100. [CrossRef]
40. Pigeon, P.; Top, S.; Vessières, A.; Huché, M.; Görmen, M.; el Arbi, M.; Plamont, M.A.; McGlinchey, M.J.; Jaouen, G.A. new series of ferrocifen derivatives, bearing two aminoalkyl chains, with strong antiproliferative effects on breast cancer cells. *New J. Chem.* **2011**, *35*, 2212. [CrossRef]
41. Tan, Y.L.K.; Pigeon, P.; Top, S.; Labbé, E.; Buriez, O.; Hillard, E.A.; Vessières, A.; Amatore, C.; Leong, W.K.; Jaouen, G. Ferrocenyl catechols: Synthesis, oxidation chemistry and anti–proliferative effects on MDA–MB–231 breast cancer cells. *Dalton Trans.* **2012**, *41*, 7537. [CrossRef]

42. Görmen, M.; Pigeon, P.; Wang, Y.; Vessières, A.; Top, S.; Martial, F.; Gros, C.; McGlinchey, M.J.; Jaouen, G. Side-Chain Effects on the 1-(Bis-aryl-methylidene)-[3]ferrocenophane Skeleton: Antiproliferative Activity against TNBC Cancer Cells and Comparison with the Acyclic Ferrocifen Series. *Eur. J. Inorg. Chem.* **2017**, *2*, 454–465. [CrossRef]
43. Acton, N.; Brossi, A.; Newton, D.L.; Sporn, M.B. Potential prophylactic antitumor activity of retinylidene 1,3–diketones. *J. Med. Chem.* **1980**, *23*, 805–809. [CrossRef] [PubMed]
44. Patra, M.; Gasser, G.; Wenzel, M.; Merz, K.; Bandow, J.E.; Metzler–Nolte, N. Sandwich and Half–Sandwich Derivatives of Platensimycin: Synthesis and Biological Evaluation. *Organometallics* **2012**, *31*, 5760–5771. [CrossRef]
45. Yan, J.; Yue, K.; Fan, X.; Xu, X.; Wang, J.; Qin, M.; Zhang, Q.; Hou, X.; Li, X.; Wang, Y. Synthesis and bioactivity evaluation of ferrocene–based hydroxamic acids as selective histone deacetylase 6 inhibitors. *J. Med. Chem.* **2023**, *246*, 115004. [CrossRef] [PubMed]
46. Mazur, M.; Mrozowicz, M.; Buchowicz, W.; Koszytkowska–Stawińska, M.; Kamiński, R.; Ochal, Z.; Wińska, P.; Bretner, M. Formylation of a metathesis–derived *ansa* [4]–ferrocene: A simple route to anticancer organometallics. *Dalton Trans.* **2020**, *49*, 11504–11511. [CrossRef]
47. Mazur, M.; Ziemkiewicz, K.; Rawiak, K.; Kisiel, K.; Wińska, P.; Deresz, K.; Jarzembska, K.N.; Buchowicz, W. N -Allyl-N-ferrocenylmethylamines and *ansa*-Ferrocenylmethylamines: Synthesis, Structure, and Biological Evaluation. *Eur. J. Inorg. Chem.* **2022**, *10*, e202101098. [CrossRef]
48. Debnath, S.; Agarwal, A.; Kumar, N.R.; Bedi, A. Selenium–Based Drug Development for Antioxidant and Anticancer Activity. *Future Pharmacol.* **2022**, *2*, 595–607. [CrossRef]
49. Zhou, H.Y.; Li, M.; Qu, J.; Jing, S.; Xu, H.; Zhao, J.Z.; Zhang, J.; He, M.F. Effective Antitumor Candidates Based upon Ferrocenylseleno–Dopamine Derivatives: Growth Inhibition by Induction Cell Apoptosis and Antivascular Effects. *Organometallics* **2016**, *35*, 1866–1875. [CrossRef]
50. Cheng, Q.; Zhou, T.; Xia, Q.; Lu, X.; Xu, H.; Hu, M.; Jing, S. Design of ferrocenylseleno–dopamine derivatives to optimize the Fenton–like reaction efficiency and antitumor efficacy. *RSC Adv.* **2021**, *11*, 25477–25483. [CrossRef]
51. Zhou, J.; Zhu, X.; Cheng, Q.; Wang, Y.; Wang, R.; Cheng, X.; Xu, J.; Liu, K.; Li, L.; Li, X.; et al. Ferrocene Functionalized Upconversion Nanoparticle Nanosystem with Efficient Near–Infrared–Light–Promoted Fenton–Like Reaction for Tumor Growth Suppression. *Inorg. Chem.* **2020**, *59*, 9177–9187. [CrossRef]
52. Qu, J.; Xia, Q.; Ji, W.; Jing, S.; Zhu, D.; Li, L.; Huang, L.; An, Z.; Xin, C.; Ni, Y.; et al. A ferrocene∩europium assembly showing phototriggered anticancer activity and fluorescent modality imaging. *Dalton Trans.* **2018**, *47*, 1479–1487. [CrossRef] [PubMed]
53. Salas, P.F.; Herrmann, C.; Cawthray, J.F.; Nimphius, C.; Kenkel, A.; Chen, J.; de Kock, C.; Smith, P.J.; Patrick, B.O.; Adam, M.J.; et al. Structural characteristics of chloroquine–bridged ferrocenophane analogues of ferroquine may obviate malaria drug–resistance mechanisms. *J. Med. Chem.* **2013**, *56*, 1596–1613. [CrossRef]
54. Vale, N.; Silva, S.; Duarte, D.; Crista, D.M.A.; Pinto da Silva, L.; Esteves da Silva, J.C.G. Normal breast epithelial MCF–10A cells to evaluate the safety of carbon dots. *RSC Med. Chem.* **2021**, *12*, 245–253. [CrossRef] [PubMed]
55. Prasad, V.V.T.S. Gopalan, Continued use of MDA–MB–435, a melanoma cell line, as a model for human breast cancer, even in year, 2014. *npj Breast Cancer* **2015**, *1*, 15002. [CrossRef]
56. Viotte, M.; Gautheron, B.; Kubicki, M.M.; Mugnier, Y.; Parish, R.v. New Iron(II)–and Gold(I)–Containing Metallocenes. X–ray Structure of a Three–Coordinate Gold(I) Ferrocenophane–Type Representative. *Inorg. Chem.* **1995**, *34*, 3465–3473. [CrossRef]
57. Ketata, E.; Neifar, A.; Mihoubi, W.; Pigeon, P.; Gouzi, H.; Mallet, J.-M.; Top, S.; Gupta, G.K.; Jaouen, G.; Gargouri, A.; et al. The inhibition of tyrosinase by some aryl butenes: A desired activity or a side effect to avoid. *J. Organomet. Chem.* **2017**, *848*, 133–141. [CrossRef]
58. Xie, Y.F.; Dou, Y.Y.; Chen, S.S.; Mi, N.; Tang, L.F. Synthesis, structure, and fungicidal activity of thia– and aza–ferrocenophanes. *J. Coord. Chem.* **2010**, *63*, 1904–1912. [CrossRef]
59. El Arbi, M.; Théolier, J.; Pigeon, P.; Jellali, K.; Trigui, F.; Top, S.; Aifa, S.; Fliss, I.; Jaouen, G.; Hammami, R. Antibacterial properties and mode of action of new triaryl butene citrate compounds. *Eur. J. Med. Chem.* **2014**, *76*, 408–413. [CrossRef]
60. Al–Bari, M.A.A.; Hossen, M.F.; Khan, A.; Islam, M.R.; Kudrat–E–Z, M.; Mosa, M.A.; Zakaria, C.M.; Islam, M.A. In vitro Antimicrobial and Cytotoxic Activities of Ferrocene Derivative Compounds. *Pak. J. Biol. Sci.* **2007**, *10*, 2423–2429. [CrossRef]
61. El Arbi, M.; Pigeon, P.; Top, S.; Rhouma, A.; Aifa, S.; Rebai, A.; Vessières, A.; Plamont, M.-A.; Jaouen, G. Evaluation of bactericidal and fungicidal activity of ferrocenyl or phenyl derivatives in the diphenyl butene series. *J. Organomet. Chem.* **2011**, *696*, 1038–1048. [CrossRef]
62. Zhang, Y.; Wang, Z.; Kouznetsova, T.B.; Sha, Y.; Xu, E.; Shannahan, L.; Fermen–Coker, M.; Lin, Y.; Tang, C.; Craig, S.L. Distal conformational locks on ferrocene mechanophores guide reaction pathways for increased mechanochemical reactivity. *Nat. Chem.* **2020**, *13*, 56–62. [CrossRef] [PubMed]
63. Peluso, P.; Mamane, V. Ferrocene derivatives with planar chirality and their enantioseparation by liquid–phase techniques. *Electrophoresis* **2023**, *44*, 158–189. [CrossRef] [PubMed]
64. Patra, M.; Gasser, G. The medicinal chemistry of ferrocene and its derivatives. *Nat. Rev. Chem.* **2017**, *1*, 0066. [CrossRef]

65. Gansane, A.; Lingani, M.; Yeka, A.; Nahum, A.; Bouyou–Akotet, M.; Mombo–Ngoma, G.; Kaguthi, G.; Barceló, C.; Laurijssens, B.; Cantalloube, C.; et al. Randomized, open–label, phase 2a study to evaluate the contribution of artefenomel to the clinical and parasiticidal activity of artefenomel plus ferroquine in African patients with uncomplicated *Plasmodium falciparum* malaria. *Malar. J.* **2023**, *22*, 2. [CrossRef]
66. Central Drugs Standard Control Organization. Available online: https://cdsco.gov.in/opencms/resources/UploadCDSCOWeb/2018/UploadCommitteeFiles/Recommendations%20%20for%20IND%20meeting%20dated%2014.02.2024.pdf (accessed on 1 August 2024).

Disclaimer/Publisher's Note: The statements, opinions and data contained in all publications are solely those of the individual author(s) and contributor(s) and not of MDPI and/or the editor(s). MDPI and/or the editor(s) disclaim responsibility for any injury to people or property resulting from any ideas, methods, instructions or products referred to in the content.